

Efficiency Separation Process of H₂/CO₂/CH₄ Mixtures by a Hollow Fiber Dual Membrane Separator

Authors:

Wu Xiao, Pei Gao, Yan Dai, Xuehua Ruan, Xiaobin Jiang, Xuemei Wu, Yuanxin Fang, Gaohong He

Date Submitted: 2020-07-17

Keywords: membrane area ratio, Optimization, ternary gas mixtures, dual membrane separator, hydrogen purification

Abstract:

Hydrogen purification and CO₂ capture are of great significance in refineries and pre-combustion power plants. A dual membrane separator offers an alternative approach for improving H₂/CO₂ separation efficiency. In this work, H₂/CO₂/CH₄ ternary gas mixtures separation can be achieved by a dual membrane separator with an integrated polyimide (PI) membrane and polydimethylsiloxane/polyetherimide (PDMS/PEI) composite membrane. A hollow fiber dual membrane separation equipment is designed and manufactured. Through the self-designed device, the effects of stage cut, operating temperature, operating pressure, and membrane area ratio on separation performance of dual membrane separator have been studied. The results indicate that, at a high stage cut, a dual membrane separator has obvious advantages over a single membrane separator. Operating temperature has a significant impact on gas permeation rates. At 25 °C, a dual membrane separator can obtain the highest purity of H₂ and CO₂. By increasing operating pressure, the purity and recovery of H₂ and CO₂ can be improved simultaneously. The effect of the membrane area ratio on the performance of the dual membrane separator was studied. When the permeate flows of two membranes are approximately equal by changing the membrane area ratio, the overall performance of the dual membrane separator is the best. On the basis of its synergy in promoting separation, the dual membrane separator holds great industrial application potential.

Record Type: Published Article

Submitted To: LAPSE (Living Archive for Process Systems Engineering)

Citation (overall record, always the latest version):

LAPSE:2020.0829

Citation (this specific file, latest version):

LAPSE:2020.0829-1

Citation (this specific file, this version):



LAPSE:2020.0829-1v1

DOI of Published Version: <https://doi.org/10.3390/pr8050560>

License: Creative Commons Attribution 4.0 International (CC BY 4.0)

Article

Efficiency Separation Process of H₂/CO₂/CH₄ Mixtures by a Hollow Fiber Dual Membrane Separator

Wu Xiao ¹, Pei Gao ¹, Yan Dai ^{1,2}, Xuehua Ruan ¹, Xiaobin Jiang ¹, Xuemei Wu ¹, Yuanxin Fang ¹ and Gaohong He ^{1,2,*}

¹ State Key Laboratory of Fine Chemicals, R&D Center of Membrane Science and Technology, School of Chemical Engineering, Dalian University of Technology, Dalian 116023, China; wuxiao@dlut.edu.cn (W.X.); gaoxiaopei@mail.dlut.edu.cn (P.G.); daiyan@dlut.edu.cn (Y.D.); xuehuan@dlut.edu.cn (X.R.); xbjiang@dlut.edu.cn (X.J.); xuemeiw@dlut.edu.cn (X.W.); fhyqx123@mail.dlut.edu.cn (Y.F.)

² Panjin Industrial Technology Institute, Dalian University of Technology, Panjin 124221, China

* Correspondence: hgaohong@dlut.edu.cn

Received: 18 April 2020; Accepted: 5 May 2020; Published: 9 May 2020



Abstract: Hydrogen purification and CO₂ capture are of great significance in refineries and pre-combustion power plants. A dual membrane separator offers an alternative approach for improving H₂/CO₂ separation efficiency. In this work, H₂/CO₂/CH₄ ternary gas mixtures separation can be achieved by a dual membrane separator with an integrated polyimide (PI) membrane and polydimethylsiloxane/polyetherimide (PDMS/PEI) composite membrane. A hollow fiber dual membrane separation equipment is designed and manufactured. Through the self-designed device, the effects of stage cut, operating temperature, operating pressure, and membrane area ratio on separation performance of dual membrane separator have been studied. The results indicate that, at a high stage cut, a dual membrane separator has obvious advantages over a single membrane separator. Operating temperature has a significant impact on gas permeation rates. At 25 °C, a dual membrane separator can obtain the highest purity of H₂ and CO₂. By increasing operating pressure, the purity and recovery of H₂ and CO₂ can be improved simultaneously. The effect of the membrane area ratio on the performance of the dual membrane separator was studied. When the permeate flows of two membranes are approximately equal by changing the membrane area ratio, the overall performance of the dual membrane separator is the best. On the basis of its synergy in promoting separation, the dual membrane separator holds great industrial application potential.

Keywords: hydrogen purification; dual membrane separator; ternary gas mixtures; optimization; membrane area ratio

1. Introduction

Hydrogen purification and CO₂ capture are vital processes in the chemical industry and integrated gasification combined cycle (IGCC) power plants [1,2]. Syngas is first produced by the steam methane reforming or coal gasification process, and then converted to a mixture containing H₂, CO₂, CH₄, CO, H₂O, and hydrocarbons by water–gas shift reaction [3,4]. Solvent absorption is the most well-developed process to capture CO₂ and obtain pure H₂ [5]. However, the concentration of CO₂ in the shifted syngas may be high (up to 45%), which would require large equipment and high energy consumption for desorption [6]. Therefore, more economical and flexible methods are desired.

Gas membrane separation has great prospects in the petrochemical industry owing to extensibility and modularity, cost efficiency, and lower energy requirement [7–9]. The first industrial gas separation membrane is a polysulfone hollow fiber membrane for H₂ separation [10]. Nowadays, H₂-selective membranes are widely used in the field of H₂/N₂ and H₂/hydrocarbon separation, which could reach

a selectivity of more than 100. H₂-selective membranes are mainly a glassy polymer for separation, following the molecular sieve mechanism. As the kinetic diameters of H₂ and CO₂ molecules are similar, currently, the H₂/CO₂ selectivity of polymer membranes is relatively low (0.5–5) [11]. In the mixed gas environment, concentration polarization and CO₂ plasticization would further weaken the selectivity. CO₂-selective membranes have also been extensively studied [12–16], but these membranes still require further experimentation before commercialization.

Dual membrane separator provides a method to improve the performance of membrane materials. By adding a reversed-selectivity membrane into the traditional single membrane separator, two gases in the feed flow are separated from different membranes at the same time. This process reduces the competition between gas molecules in gas mixtures. Moreover, timely separation of plastic gases such as CO₂ also reduces the plasticization of membrane material.

Dual membrane separator was first proposed in the 1970s, and has since been studied by many researchers [17–23]. Ohno et al. [17] carried out an analytical study of dual membrane separator operating under “perfect mixing” conditions. It took the form of sealed retentate side, which was not conducive to industrial application. Perrin et al. [18] established a mathematical model that considered the residual side, and was applicable to three types of flow patterns, which were “perfect mixing”, countercurrent flow, and cocurrent flow. Chen et al. [19,20] embedded the models of dual membrane separator in the simulator using the User Extension interface of UniSim Design. Then, the dual membrane separator can be used for process simulation. Integrated with condensation, the dual membrane separator could be applied to light hydrocarbon recovery and natural gas pretreatment processes. In addition to numerical studies, experimental studies of dual membrane separators are also underway. Perrin et al. [21] confirmed the accuracy of the model through the experiment of He/CH₄ separation. Sengupta et al. [22] extended the numerical analysis and experimental research of the dual membrane separator to the ternary mixed gas separation process. The effects of feed composition, membrane selectivity, and flow pattern, among others, on the performance of the dual membrane separator were investigated during the separation of He/CO₂/N₂. In addition to gas separation, the dual membrane concept was applied to gas–liquid contactors [23]. Our previous simulation studies indicated that the co (H₂): counter (CO₂) dual membrane separator was an effective module configuration [24]. However, some assumptions and simplifications are usually made to the membrane separator during simulation, such as ignoring the effects of concentration polarization in the separator, gas diffusion in the flow direction, flow non-uniformity, and temperature. The expansion based on numerical results requires further experimental verification. Therefore, it is necessary to systematically study the actual separation performance and the effects of various parameters on the separation performance of dual membrane separator using experimental methods.

In this work, a hollow fiber dual membrane separator was optimized through experimental methods. The effects of process parameters (including stage cut, operating temperature, operating pressure, and membrane area ratio) on the separation performance of the dual membrane separator were investigated.

2. Materials and Methods

2.1. Preparation of Polyimide (PI) and Polydimethylsiloxane/Polyetherimide (PDMS/PEI) Hollow Fiber Membrane

Polyimide (PI) hollow fiber membranes were provided by Dalian Eurofilm Industrial Ltd. Co (Dalian, China), and PEI hollow fiber substrates used in this study were provided by Panjin Industrial Technology Institute of Dalian University of Technology (Panjin, China). Polydimethylsiloxane (PDMS) with a number average molecular weight of about 1,000,000 g mol⁻¹ was obtained from Wacker Chemicals South Asia Pte. Ltd. (Guangzhou, China). I-octane (Reagent grade) was purchased from Tianjin Fuchen Chemical Reagents Co. Ltd. (Tianjin, China). The polysiloxane containing SiH functional groups used as the cross-linker and platinum divinyl-tetramethylsiloxane complex used as the catalyst were provided by Shenzhen Kejunchi Co. Ltd. (Shenzhen, China).

PDMS/PEI hollow fiber composite membranes were prepared by the wet membrane dip-coating method [25]. Coating solution was prepared by dissolving the PDMS polymer resin, cross-linking agent, and catalyst with a weight ratio of 50:5:1 (w/w/w) in *i*-octane at room temperature to obtain a homogeneous solution. The water of PEI substrates surface was removed by filter paper, and then the wet membrane was submerged in PDMS coating solution. After the membranes were withdrawn and additional solution was dripped off, the composite membranes were cured in an oven for 2 h at 85 °C to complete PDMS cross-linking. The cross-sectional morphologies of the membranes were observed by field-emission scanning electron microscope (FE-SEM, Hitachi S4800, Tokyo, Japan).

2.2. Design and Packaging of Dual Membrane Separator

As shown in Figure 1, the dual membrane separator used in this study consisted of a stainless steel casing and two aluminum head. One side of several hollow fiber membranes was bundled with absorbent cotton, put into aluminum heads, and then sealed with epoxy resin. The other side of the membranes was blocked with epoxy resin. To assemble a dual membrane separator, the two heads equipped with PDMS/PEI hollow fiber membranes and PI hollow fiber membranes needed to be placed at the two ends of the stainless steel casing, respectively, and sealed by O-rings and flanges. The separator was connected to test the system to study its gas separation performance. The head of the PI membranes can be taken out for testing as a PDMS/PEI single membrane separator, and vice versa.

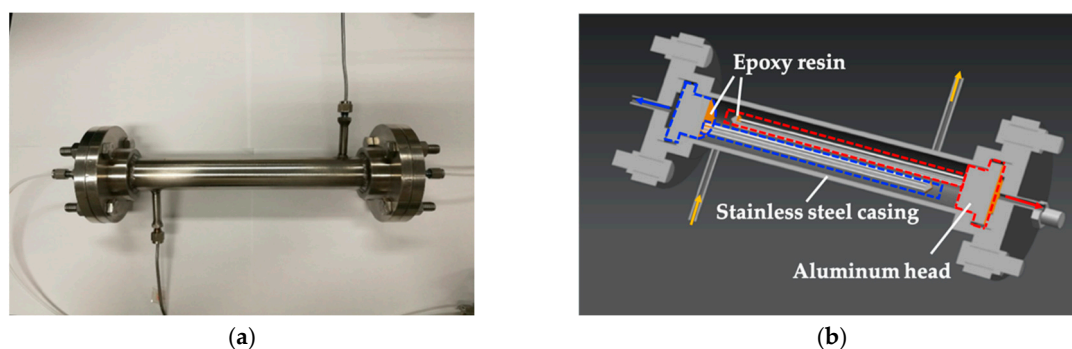


Figure 1. Dual membrane separator (a) Appearance of dual membrane separator; (b) internal structure diagram.

2.3. Experimental Set-Up and Analysis System

Permeation and separation experiments were carried out in the setup represented schematically in Figure 2. The feed was introduced and removed from the shell. PI membranes permeate and feed kept a co-current flow pattern, while PDMS/PEI membranes kept a countercurrent flow pattern. The feed pressure and flow were adjusted by a pressure regulator and a back pressure regulator. The separator was immersed in a thermostatic water bath. The gas permeate or retentate volumetric flow rate was measured by a soap bubble flow meter. The design of the inlet section offered the possibility of testing pure and mixed gases. The pure gas permeation experiments were conducted under the operating conditions of 0.2 MPa feed pressure and 25 °C. The retentate was plugged and only the flow rate of permeate streams was measured. The pure gas test data could be used to determine the quality of the package and membranes. In the mixed gas experiment, in order to simulate syngas for water–gas shift reaction, H₂/CO₂/CH₄ three-component gas mixtures with a molar ratio of 45:40:15 were used as feed gas. This process required an opened retentate and the flow rates and composition of the two permeates and the retentate needed to be measured. The gas composition of each pipeline was analyzed by gas chromatography equipped with TCD (Thermal conductivity detector) and FID (Flame ionization detector) dual detectors (GC 7900, Techcomp Scientific Instruments Co., Ltd., Shenyang, China), and three samples were taken at each sampling point. Before starting the experiment, the pipeline was purged with nitrogen for 10 min. After changing the gas, sufficient purge was also

required to eliminate the effect of the previous gas on the membrane material, and the recording was started after the flow rate and composition were stable.

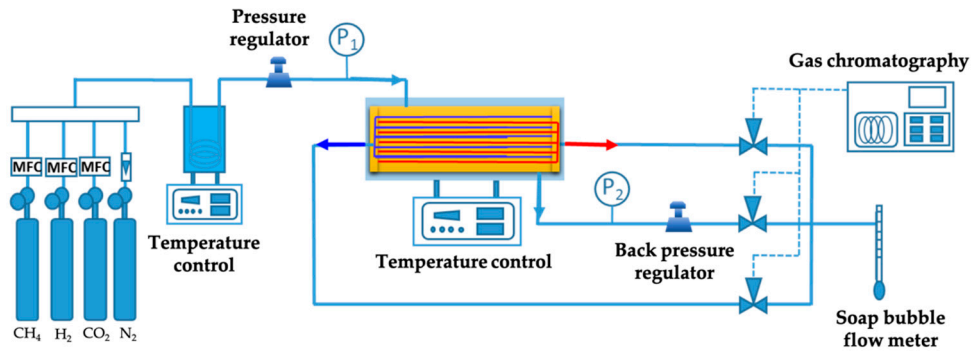


Figure 2. Schematic of the dual membrane separator experimental setup.

2.4. Theoretical Analysis

The performances of the membranes were evaluated in terms of the permeation rate and the separation factor.

The permeability of pure gas i is determined by the following equation:

$$J_i = \frac{Q_P}{A(p_F - p_P)} \quad (1)$$

The permeability of gas i in the mixed gas is determined by the following equation:

$$J_i = \frac{Q_P y_i}{A(p_F k_i - p_P y_i)} \quad (2)$$

$$k_i = \frac{f_i + x_i}{2} \quad (3)$$

where J_i is the permeation rate GPU (Gas permeation unit), $\text{GPU} = 10^{-6} \times \text{cm}^3 \cdot \text{cm}^{-2} \cdot \text{s}^{-1} \cdot \text{cmHg}^{-1}$; Q_P is the gas permeate volumetric flow rate ($\text{cm}^3 \cdot \text{s}^{-1}$); A is membrane effective surface area (cm^2); p_F and p_P are the pressure on the feed and permeate, respectively (cmHg); and f_i , x_i , and y_i are the mole fractions of gas component i on the feed, retentate, and permeate, respectively.

$\alpha_{A/B}$, as the selectivity of gas pair A/B, is defined as the ratio of the gas permeation rate of two gases, which is represented as below.

$$\alpha_{A/B} = \frac{J_A}{J_B} \quad (4)$$

The separation efficiency of the membrane separator is expressed by the purity and recovery of the product. Dual membrane separator can obtain two enriched products at the same time: H_2 product is obtained on the permeation side of PI membranes, and CO_2 product is obtained on the permeation side of PDMS/PEI membranes.

The recovery of gas φ_R on the permeate sides:

$$Q_F = Q_P + Q_R \quad (5)$$

$$\varphi_R = \frac{Q_P \times y_i}{Q_F \times f_i} \quad (6)$$

where Q_F and Q_R are the feed and retentate volumetric flow rate, respectively ($\text{cm}^3 \cdot \text{s}^{-1}$).

The stage cut θ is defined as the relative magnitude between permeate and feed flow rate, which can be calculated by the following equation:

$$\theta = \frac{Q_P}{Q_F} \quad (7)$$

The membrane area ratio R is an important parameter of the dual membrane separator:

$$R = \frac{A^I}{A^{II}} \quad (8)$$

where I stands for PI membranes and II stands for PDMS/PEI membranes.

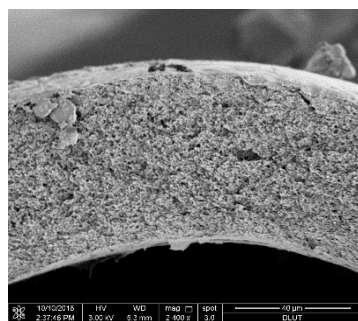
3. Results and Discussion

3.1. Basic Properties of the Two Hollow Fiber Membranes

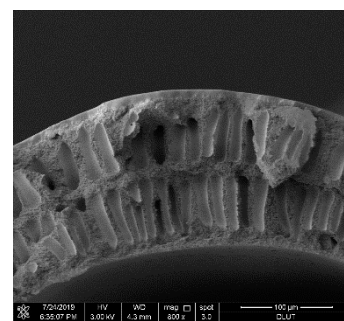
In this experiment, industrial PI hollow fiber membranes and self-made PDMS/PEI hollow fiber composite membranes were used. On the basis of the pure gas tests, the permeances and ideal selectivities were calculated. The results are summarized in Table 1. Compared with other gases, H_2 through PI membranes and CO_2 through PDMS/PEI membranes have the highest permeances. The cross-section micrographs of the PI membranes and PDMS/PEI composite membranes are shown in Figure 3. The PI displays sponge-like voids from Figure 3a. The PEI substrate displays finger-like voids originating from the inner and outer surfaces from Figure 3b. PDMS can be found well attached to the PEI hollow substrate forming uniform PDMS layers. These results reflect physicochemical properties of the particular polymer: PI is glassy, while PDMS is rubbery [25,26]. For glassy polymers, the mass transfer mainly depends on diffusion selectivity and smaller molecules preferentially pass the membrane. By contrast, solubility predominates the mass transfer through rubbery CO_2 -philic polymers such as PDMS.

Table 1. Performance parameters of polyimide (PI) and polydimethylsiloxane/polyetherimide (PDMS/PEI) hollow fiber membranes.

25 °C, 0.2 MPa	Outer Diameter/ μm	Internal Diameter/ μm	J/GPU (Gas Permeation Unit)			α	
			H_2	CO_2	CH_4	H_2/CO_2	CO_2/H_2
PI	333	186	148	32	1	4.6	-
PDMS/PEI	939	592	50	163	45	-	3.3



(a)



(b)

Figure 3. Scanning electron microscope (SEM) images of the cross-section structure of the two hollow fiber membranes. (a) Polyimide (PI) hollow fiber membrane; (b) polydimethylsiloxane/polyetherimide (PDMS/PEI) hollow fiber composite membrane.

3.2. Parameter Optimization of PI/PDMS Dual Membrane Separator

3.2.1. Effect of Stage Cut

Figure 4 shows the influence of stage cut on the traditional PI membrane separator and PI/PDMS dual membrane separator at feed pressure of 0.2 MPa and operating temperature of 25 °C. It could be observed that H₂ purity (y_{H_2}) decreased with the increase of stage cut in the PI membrane separator. At a high stage cut, most of the feed permeated through the membranes, which means a high H₂ recovery. However, it also resulted in the similar concentration of feed and permeate stream. Therefore, the driving force for H₂ permeation was reduced and H₂ purity decreased. However, this phenomenon was not so obvious in the dual membrane separator. Because PDMS/PEI membranes in the dual membrane separator removed CO₂ from feed gas, CO₂ concentration (x_{CO_2}) in the retentate side was significantly reduced, thereby increasing the driving force for H₂ permeation through PI membranes. Thanks to its enhanced separation, dual membrane separator could simultaneously obtain products with higher purity and higher recovery.

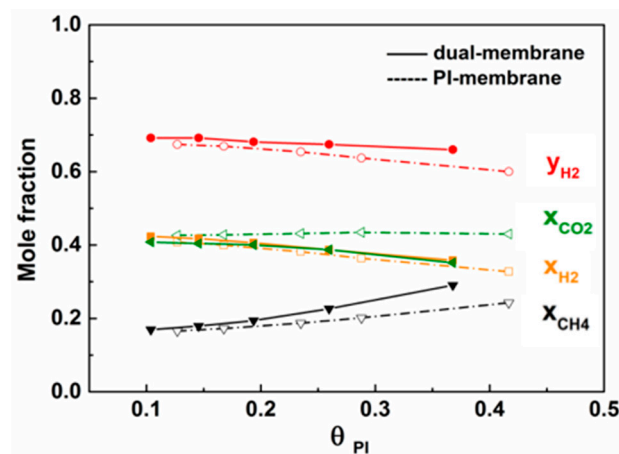


Figure 4. Effects of stage cut on performance of PI membrane separator and PI/PDMS dual membrane separator.

3.2.2. Effect of Operating Temperature

The mixed gas experiments were carried out to investigate the effects of operating temperature on PI and PDMS/PEI membrane performances. The results were obtained at 0.2 MPa and a temperature range of 25–65 °C. As shown in Figure 5a, with the increase of temperature, the permeation rate of all gases through PI membranes increased. From 25 °C to 65 °C, H₂ and CO₂ permeation rate increased by 81% and 104%, respectively. As a result, the selectivity of H₂/CO₂ decreased by 11%. In the glassy PI membrane, the diffusion coefficient plays a major role and its temperature dependence follows Arrhenius's law [27]. Large gas molecules require high diffusion activation energy and are more sensitive to temperature. So, the increase of CO₂ permeation rate was greater than that of H₂. However, CO₂ was less affected by temperature in PDMS/PEI membranes (Figure 5b). The effect of temperature on gas permeation rate can also be described by an Arrhenius relationship. CO₂ is a condensable gas, and the apparent activation energy in rubbery polymers is often lower than that of H₂ and CH₄ [25]. As the temperature increases, the permeation rate of H₂ increased significantly, and CO₂/H₂ selectivity in PDMS/PEI membranes decreased.

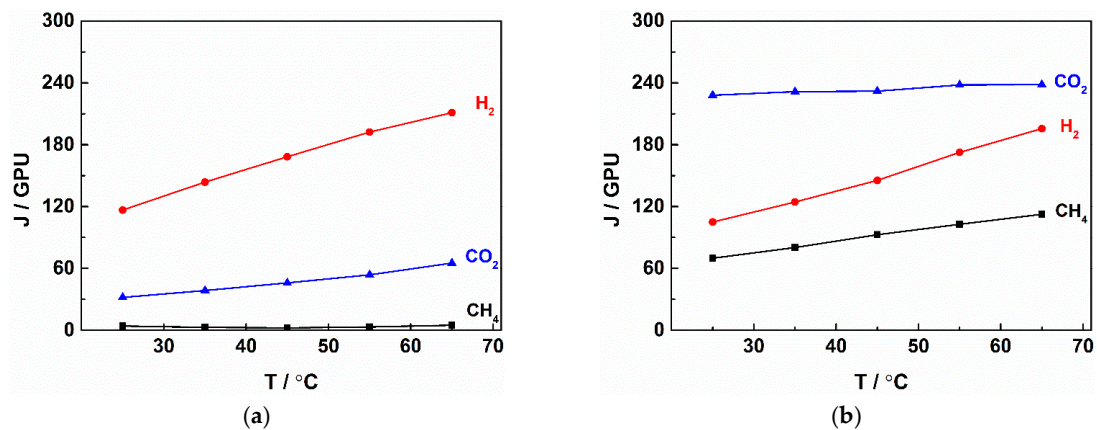


Figure 5. Effects of operating temperature on membrane performances. (a) PI membrane gas permeation rates; (b) PDMS/PEI membrane gas permeation rates.

Figure 6 depicts the effect of operating temperature on the purity and recovery of dual membrane separator. It could be observed from Figure 6a that as the temperature rose from 25 °C to 65 °C, H₂ recovery increased by about 46%, while the CO₂ recovery remained basically unchanged. This was consistent with the effects of temperature on the permeation rates of the two membranes. The increase of gas permeation rate in the membrane could bring a certain increase in gas recovery. Thus, increasing operating temperature is beneficial to improve H₂ recovery of the dual membrane separator. As shown in Figure 6b, the purity of H₂ and CO₂ both showed a downward trend. It was mainly caused by the decrease in the selectivities of H₂/CO₂ of PI membranes and CO₂/H₂ of PDMS/PEI membranes at higher temperatures. The increase of the CH₄ permeation rate would also reduce the purity of H₂ and CO₂.

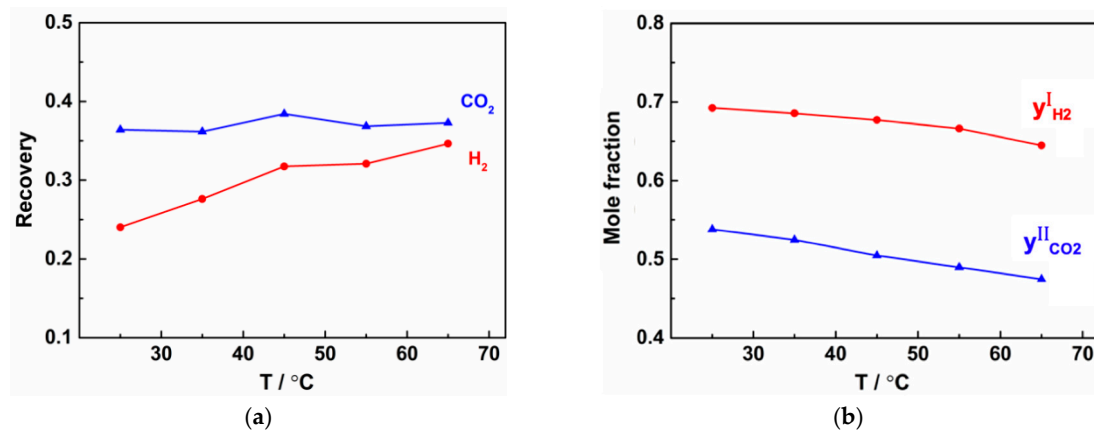


Figure 6. Effects of operating temperature on the purity and recovery of dual membrane separator. (a) The recovery of H₂ and CO₂; (b) the purity of H₂ and CO₂.

In industry, product recovery can be improved by increasing the stage cut, but it is relatively difficult to improve product purity. Therefore, selecting a lower temperature (such as 25 °C in this experiment) to ensure higher purity is more beneficial to the application of the dual membrane separator.

3.2.3. Effect of Operating Pressure

The presence of CO₂ in the feed gas made the polymer matrix easily plasticized, which resulted in an increase in gas permeation rate. As the pressure increased, the polymer matrix tended to be plasticized strongly [28,29]. Figure 7 illustrated the effects of operating pressure on PI and PDMS/PEI membrane properties at 25 °C and a pressure range of 0.2–0.8 MPa. The permeation rates of H₂, CO₂, and CH₄ by PI membranes were almost independent of the operating pressure, as shown in Figure 7a.

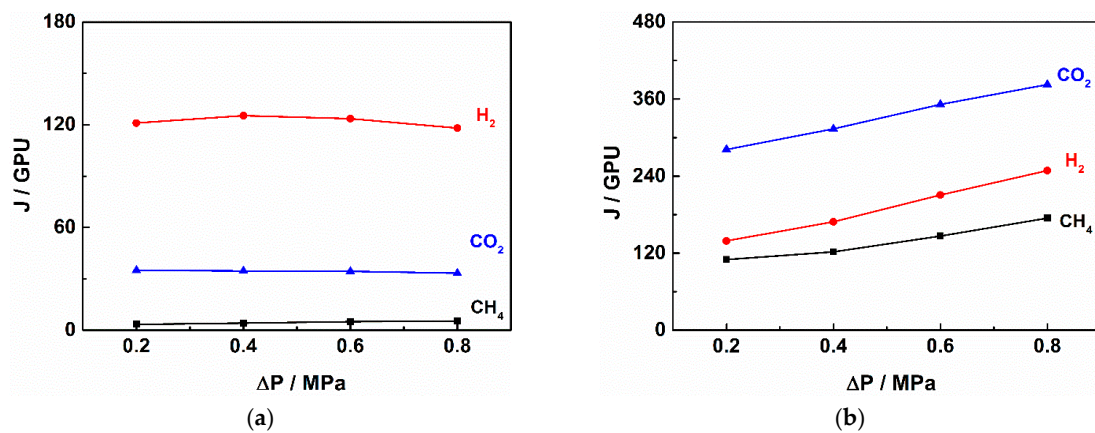


Figure 7. Effects of operating pressure on membrane performances. (a) PI membrane gas permeation rates; (b) PDMS/PEI membrane gas permeation rates.

The results indicated that the industrialized PI membranes used in this study had a good ability to resist plasticizing. However, CO_2 had higher solubility in the PDMS membrane. As shown in Figure 7b, in PDMS/PEI membranes, the permeation rates of all three gases increased with the operating pressure.

Figure 8 shows the effect of operating pressure on the purity and recovery of the dual membrane separator. As is known to us, there is a clear trade-off relationship between recovery and purity in conventional single membrane separators. It was worth noting that, in the dual membrane separator, with the increase of operating pressure, the purity and recovery of H_2 and CO_2 increased simultaneously. This results fully reflected the enhanced separation effect of the dual membrane separator. The increase of CO_2 permeation rate in PDMS/PEI membranes helps reduce the CO_2 concentration in feed, and which leads to a larger driving force for H_2 to permeate through PI membranes. At the same time, more H_2 passed through the PI membranes, temporarily eliminating the effect of the PDMS/PEI membranes selectivity decline.

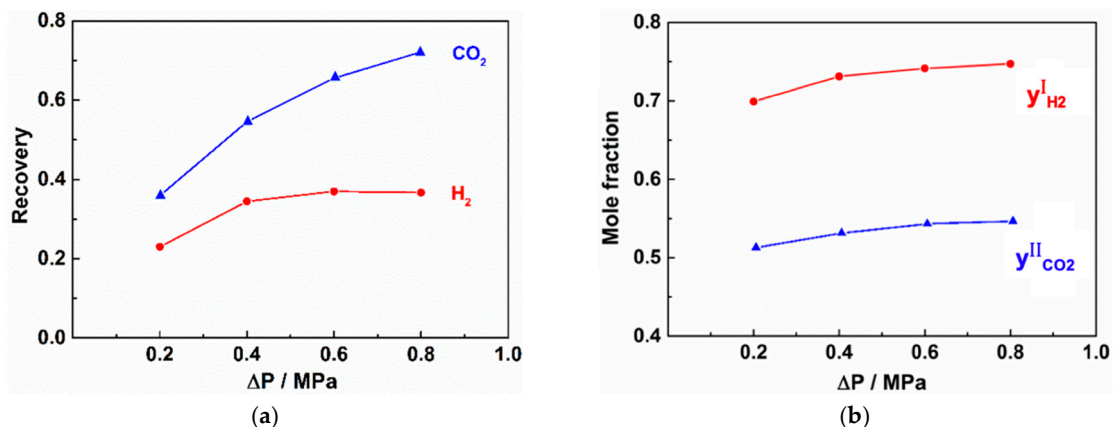


Figure 8. Effects of operating pressure on the purity and recovery of the dual membrane separator. (a) The recovery of H_2 and CO_2 ; (b) the purity of H_2 and CO_2 .

Therefore, a higher operating pressure is beneficial to the separation of the dual membrane separator. Certainly, the optimization of operating pressure should also consider the impact of compressor energy consumption and the pressure resistance of the hollow fiber in the separator.

3.2.4. Effect of Membrane Area Ratio

The area ratio of the two membranes was a critical parameter in a dual membrane separator. Figure 9 presented the influence of membrane area ratio (R) on membrane separation performance

at different feed rates. The external separation efficiency of the dual membrane separator is closely related to the performance of the internal membrane material. Therefore, a fixed flow rate (100 mL/min) in Figure 9a,b was selected. At this point, the permeation rate and selectivity of the PI membrane in the dual membrane separator are shown in Table 2.

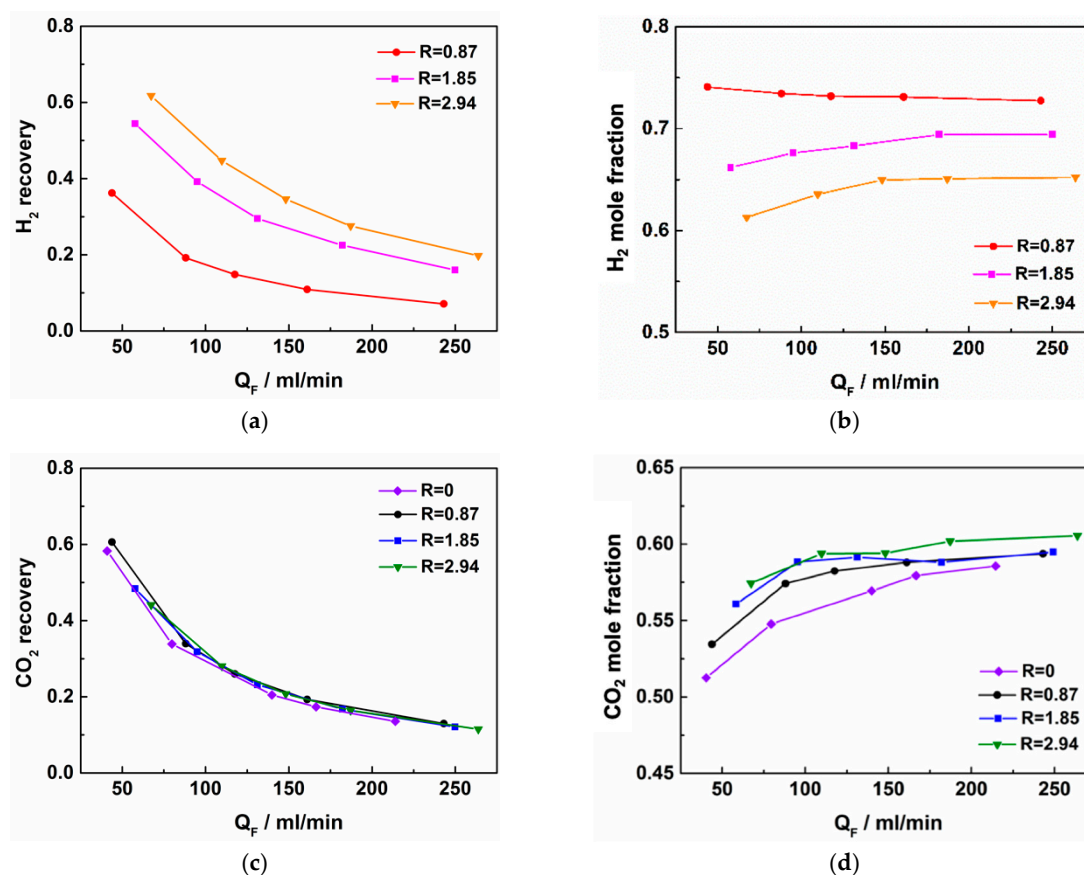


Figure 9. Effects of membrane area ratio on separation performance of dual membrane separator. (a) The recovery of H_2 ; (b) the purity of H_2 ; (c) the recovery of CO_2 ; and (d) the purity of CO_2 .

Table 2. Performance of PI membranes in the dual membrane separator under different membrane area ratios (Q_F was about 100 mL/min).

R	J/GPU			α
	H_2	CO_2	CH_4	H_2/CO_2
0.87	123	28	1	4.4
1.85	128	38	3	3.3
2.94	100	35	7	2.8

Mixed gas experiments were carried out at 25 °C and 0.2 MPa. The area of PDMS/PEI membranes was fixed, and R could be adjusted by changing the area of PI membranes. As illustrated in Figure 9a,b, a trade-off could also be found between the H_2 recovery and purity. When R increased from 0.87 to 2.94, H_2 recovery increased from 0.15 to 0.45 and H_2 purity dropped by about 12% at a feed flow rate of 100 mL/min. Figure 9c,d showed the trade-off of CO_2 purity and recovery on the PDMS/PEI membranes. “R = 0” implied that there was only a PDMS/PEI membrane in the separator.

The effect of the membrane area ratio on the dual membrane separator can be explained by the matching of gas permeability of PI membranes and PDMS/PEI membranes. When R was 2.94, most of the feed permeated through PI membranes, which resulted in the highest recovery of H_2 (Figure 9a). The H_2 purity and H_2/CO_2 selectivity of PI membranes in the dual membrane separator were similar to

the single PI membrane separator (Table 2: $R = 2.94$). When R was 1.85, recovery of the two membranes was approximately equal. As R decreased to 1.85, PDMS/PEI membranes showed a greater impact on gas composition of the high-pressure side in the separator, which led to an increase in H_2 permeability of PI membranes and an increase in the purity of H_2 products. At this time, the increase of feed rate would further strengthen the convection and accelerate the H_2 enrichment. At a 100 ml/min feed flow rate, the recovery of H_2 was about 0.40, and the purity was 0.67. When R was 0.87, most of the feed permeated through PDMS/PEI membranes, which led to the lowest recovery of H_2 and the reduction of the H_2 permeation rate through PI membranes (Table 2: $R = 0.87$). In this case, enough feed in the separator was diffused to the surface of PI membranes, and the control step of separation changed from the process of gas diffusion to the membrane surface to the process of gas permeation through the membrane. The latter process was determined by the membrane, so at this time, the selectivity of H_2/CO_2 of PI membranes was close to the value of the pure gas test (about 4.6). Meanwhile, the purity of the H_2 product was the highest. In this condition, the feed rate increased, and more feed gas entered the retentate, which caused the H_2 purity to decrease (Figure 9b). Similar results were obtained on PDMS/PEI membranes, but as the membrane area of PDMS/PEI remained unchanged, the absolute change was not much (Figure 9c,d).

Although the H_2/CO_2 selectivity of PI membranes and the purity of the H_2 product were the highest when R was 0.87, the recovery of H_2 decreases greatly. Considering the recovery rate and purity of H_2 comprehensively, the membrane area ratio of 1.85 is the best choice.

4. Conclusions

A PI/PDMS hollow fiber dual membrane separator was designed and applied to separate ternary gas mixtures. Higher gas separation performance could be achieved by adjusting various process parameters to match the permeability and selectivity of the two membranes. The membrane area ratio was a system parameter of the dual membrane separator, which could be used to adjust the purity and recovery of the single-sided product. With R increased, a higher H_2 recovery could be achieved, but also a lower H_2 purity. When R was 1.85, which means permeation of the two membranes was approximately equal, the dual membrane separator could have the best overall performance of the separation. At a high stage cut, the dual membrane separator effectively reduced the concentration polarization by reducing the CO_2 concentration in feed gas, and the product purity was significantly improved compared with the PI single membrane separator. A high temperature was detrimental to the products' purity of the dual membrane separator. In order to obtain high purity products, the optimal temperature should be 25 °C. With the increase of operating pressure, the purity and recovery of H_2 and CO_2 increased at the same time. According to the requirements of industrial production, a higher operating pressure was preferred. The dual membrane separator is expected to play an important role in the recovery of H_2 and the reduction of greenhouse gases.

Author Contributions: Conceptualization, W.X. and P.G.; methodology, Y.D. and X.R.; investigation, X.J. and X.W.; writing—original draft preparation, P.G. and W.X.; writing—review and editing, P.G. and W.X.; visualization, Y.F. supervision, G.H.; project administration, G.H.; funding acquisition, G.H. All authors have read and agreed to the published version of the manuscript.

Funding: Joint Funds of the National Natural Science Foundation of China (U1663223), the National Natural Science Foundation of China (Grant No. 21776034, 21676043, 21706023), MOST innovation team in key area (No. 2016RA4053), the Major National Scientific Instrument Development Project (21527812), and Education Department of the Liaoning Province of China (LT2015007).

Acknowledgments: The authors are grateful to the foundations and the education department for their support.

Conflicts of Interest: The authors declare no conflict of interest.

References

1. Giordano, L.; Gubis, J.; Bierman, G.; Kapteijn, F. Conceptual design of membrane-based pre-combustion CO₂ capture process: Role of permeance and selectivity on performance and costs. *J. Membr. Sci.* **2019**, *575*, 229–241. [[CrossRef](#)]
2. Merkel, T.C.; Zhou, M.; Baker, R.W. Carbon dioxide capture with membranes at an IGCC power plant. *J. Membr. Sci.* **2012**, *389*, 441–450. [[CrossRef](#)]
3. Dou, B.; Zhang, H.; Song, Y.; Zhao, L.; Jiang, B.; He, M.; Ruan, C.; Chen, H.; Xu, Y. Hydrogen production from the thermochemical conversion of biomass: Issues and challenges. *Sustain. Energy Fuels* **2019**, *3*, 314–342. [[CrossRef](#)]
4. Chen, B.; Yang, T.; Xiao, W.; Nizamani, A.K. Conceptual design of pyrolytic oil upgrading process enhanced by membrane-integrated hydrogen production system. *Processes* **2019**, *7*, 284. [[CrossRef](#)]
5. Wang, R.; Liu, S.; Wang, L.; Li, Q.; Zhang, S.; Chen, B.; Jiang, L.; Zhang, Y. Superior energy-saving splitter in monoethanolamine-based biphasic solvents for CO₂ capture from coal-fired flue gas. *Appl. Energy* **2019**, *242*, 302–310. [[CrossRef](#)]
6. Lin, H.; He, Z.; Sun, Z.; Kniep, J.; Ng, A.; Baker, R.W.; Merkel, T.C. CO₂-selective membranes for hydrogen production and CO₂ capture—Part II: Techno-economic analysis. *J. Membr. Sci.* **2015**, *493*, 794–806. [[CrossRef](#)]
7. Chen, X.; Kaliaguine, S.; Rodrigue, D. Correlation between performances of hollow fibers and flat membranes for gas separation. *Sep. Purif. Rev.* **2018**, *47*, 66–87. [[CrossRef](#)]
8. Baker, R.W.; Lokhandwala, K. Natural gas processing with membranes: An overview. *Ind. Eng. Chem. Res.* **2008**, *47*, 2109–2121. [[CrossRef](#)]
9. Baker, R.W.; Low, B.T. Gas separation membrane materials: A perspective. *Macromolecules* **2014**, *47*, 6999–7013. [[CrossRef](#)]
10. Mores, P.L.; Arias, A.M.; Scenna, N.J.; Caballero, J.A.; Mussati, S.F.; Mussati, M.C. Membrane-based processes: Optimization of hydrogen separation by minimization of power, membrane area, and cost. *Processes* **2018**, *6*, 221. [[CrossRef](#)]
11. Chung, T.S.; Shao, L.; Tin, P.S. Surface modification of polyimide membranes by diamines for H₂ and CO₂ separation. *Macromol. Rapid Commun.* **2006**, *27*, 998–1003. [[CrossRef](#)]
12. Zhang, L.; Wang, X.; Yu, R.; Li, J.; Hu, B.; Yang, L. Hollow fiber membrane separation process in the presence of gaseous and particle impurities for post-combustion CO₂ capture. *Int. J. Green Energy* **2017**, *14*, 15–23. [[CrossRef](#)]
13. Ramasubramanian, K.; Zhao, Y.N.; Ho, W.S.W. CO₂ capture and H₂ purification: Prospects for CO₂-selective membrane processes. *AIChE J.* **2013**, *59*, 1033–1045. [[CrossRef](#)]
14. Song, C.; Sun, Y.; Fan, Z.; Liu, Q.; Ji, N.; Kitamura, Y. Parametric study of a novel cryogenic-membrane hybrid system for efficient CO₂ separation. *Int. J. Greenh. Gas Control* **2018**, *72*, 74–81. [[CrossRef](#)]
15. Clarizia, G.; Algieri, C.; Drioli, E. Filler-polymer combination: A route to modify gas transport properties of a polymeric membrane. *Polymer* **2004**, *45*, 5671–5681. [[CrossRef](#)]
16. Ding, M.; Flaig, R.; Jiang, H.; Yaghi, O. Carbon capture and conversion using metal-organic frameworks and MOF-based materials. *Chem. Soc. Rev.* **2019**, *48*, 2783–2828. [[CrossRef](#)]
17. Ohno, M.; Ozaki, O.; Sato, H. Radioactive rare-gas separation using a separation cell with two kinds of membrane differing in gas permeability tendency. *J. Nucl. Sci. Technol.* **1977**, *14*, 589–602. [[CrossRef](#)]
18. Perrin, J.E.; Stern, S.A. Modeling of permeators with two different types of polymer membranes. *AIChE J.* **1985**, *31*, 1167–1177. [[CrossRef](#)]
19. Chen, B.; Ruan, X.; Xiao, W.; Jiang, X.; He, G. Synergy of CO₂ removal and light hydrocarbon recovery from oil-field associated gas by dual-membrane process. *J. Nat. Gas Sci. Eng.* **2015**, *26*, 1254–1263. [[CrossRef](#)]
20. Chen, B.; Jiang, X.; Xiao, W.; Dong, Y.; Hamouti, I.E.; He, G. Dual-membrane natural gas pretreatment process as CO₂ source for enhanced gas recovery with synergy hydrocarbon recovery. *J. Nat. Gas Sci. Eng.* **2016**, *34*, 563–574. [[CrossRef](#)]
21. Perrin, J.E.; Stern, S.A. Separation of a helium-methane mixture in permeators with two types of polymer membranes. *AIChE J.* **1986**, *32*, 1889–1901. [[CrossRef](#)]
22. Sengupta, A.; Sirkar, K.K. Ternary gas mixture separation in two-membrane permeators. *AIChE J.* **1987**, *33*, 529–539. [[CrossRef](#)]

23. Cai, J.J.; Hawboldt, K.; Abdi, M.A. Improving gas absorption efficiency using a novel dual membrane contactor. *J. Membr. Sci.* **2016**, *510*, 249–258. [[CrossRef](#)]
24. Chen, B.; Ruan, X.; Jiang, X.; Xiao, W.; He, G. Dual-membrane module and its optimal flow pattern for H₂/CO₂ separation. *Ind. Eng. Chem. Res.* **2016**, *55*, 1064–1075. [[CrossRef](#)]
25. Dai, Y.; Ruan, X.; Bai, F.; Yu, M.; Li, H.; Zhao, Z.; He, G. High solvent resistance PTFPMS/PEI hollow fiber composite membrane for gas separation. *Appl. Surf. Sci.* **2016**, *360*, 164–173. [[CrossRef](#)]
26. Sanders, D.F.; Smith, Z.P.; Guo, R.; Robeson, L.M.; McGrath, J.E.; Paul, D.R.; Freeman, B.D. Energy-efficient polymeric gas separation membranes for a sustainable future: A review. *Polymer* **2013**, *54*, 4729–4761. [[CrossRef](#)]
27. Koros, W.J.; Fleming, G.K. Membrane-based gas separation. *J. Membr. Sci.* **1993**, *83*, 1–80. [[CrossRef](#)]
28. Liu, L.; Jiang, N.; Burns, C.M.; Feng, X.S. Substrate resistance in composite membranes for organic vapour/gas separations. *J. Membr. Sci.* **2009**, *338*, 153–160. [[CrossRef](#)]
29. Choi, S.H.; Kim, J.H.; Lee, S.B. Sorption and permeation behaviors of a series of olefins and nitrogen through PDMS membranes. *J. Membr. Sci.* **2007**, *299*, 54–62. [[CrossRef](#)]



© 2020 by the authors. Licensee MDPI, Basel, Switzerland. This article is an open access article distributed under the terms and conditions of the Creative Commons Attribution (CC BY) license (<http://creativecommons.org/licenses/by/4.0/>).